Methanation of Syngas over Ni-Based Catalysts with Different Supports

Buyan-Ulzii Battulga, Munkhdelger Chuluunsukh, Enkhsaruul Byambajav

Laboratory of Clean Energy Technology Development, School of Arts & Sciences, National University of Mongolia, Ulaanbaatar, Mongolia
Email: battulgabuyanaa@gmail.com

Abstract

CO methanation over the 20% nickel catalyst prepared by impregnation-precipitation method on different supports of commercial γ-Al_2O_3, TiO_2, SiO_2 and nano-γ-$Al_2O_3{}^\star$ was investigated. The nano-γ-$Al_2O_3{}^\star$ support was pulverized using a ball milling method. Catalyst characterization was done using the methods of BET, XRD, SEM, ICP-OES methods. Carbon monoxide methanation process was carried out at the temperature of 350°C in pressure of 3 bar of H_2:CO syngas with the molar ratio of 3:1 and with the GHSV of 3000 h^{-1} in a fixed bed reactor. The initial temperature of methane formation increased according to the order of Ni/γ-$Al_2O_3{}^\star$ < Ni/SiO_2 < Ni/γ-TiO_2 < Ni/γ-Al_2O_3. The Ni/γ-$Al_2O_3{}^\star$, which was prepared on the surface of nano milled γ-Al_2O_3 support, produced methane from the lowest temperature of 178°C to 350°C in CO methanation. The Ni/γ-$Al_2O_3{}^\star$ catalyst gave the highest amount of methane (0.1224 mmol/g-cat) for 1 h methanation among other catalysts. XRD and SEM analysis proved that NiO particles in the Ni/γ-$Al_2O_3{}^\star$ were finely distributed, and their sizes were smaller compared to those in the traditional one. The pulverization of γ-Al_2O_3 improved the dispersion of catalytic active nickel species inside porosity of the support leading to the improvement of its catalytic performance for CO methanation.
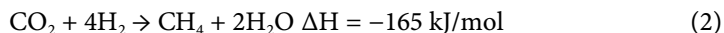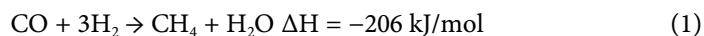
Keywords

CO Hydrogenation, Water-Gas Shift Reaction, Nano-γ-Al_2O_3, Methane Productivity

1. Introduction

Synthetic natural gas (SNG) as a clean energy carrier has been attracted increasing attention worldwide owing to its lower emissions of sulfur, nitrogen and dust

than that of direct using coal and is expected to be one of the main energy sources in the 21st century [1]. This process mainly includes coal gasification to syngas and methanation of syngas, in which methanation is a critical step with the reactions as shown in Equation (1) and Equation (2) [2].

$$CO + 3H_2 \rightarrow CH_4 + H_2O \quad \Delta H = -206 \text{ kJ/mol} \tag{1}$$

$$CO_2 + 4H_2 \rightarrow CH_4 + 2H_2O \quad \Delta H = -165 \text{ kJ/mol} \tag{2}$$

Rhodium, ruthenium and nickel are known to be catalytically active for CO and CO_2 methanation reaction. However, nickel is estimated as the most suitable commercial catalyst because of its reasonable cost and high selectivity [3] [4] [5]. The activity of Ni based catalyst can be affected by support types, preparation methods and promoters [6]-[13]. MgO, Al_2O_3, SiO_2, TiO_2 and ZrO_2 are used as a catalyst support for Ni catalyst in methanation; and these supports can affect the activities of methanation catalyst through changing the particles size and distribution of Ni active component [6]. Takenaka *et al.* [10] reported that the activity of supported Ni catalysts for CO methanation was strongly dependent on the type of catalytic supports, and the observed conversions of CO at 526 K were higher in the order of $Ni/MgO < Ni/Al_2O_3 < Ni/SiO_2 < Ni/TiO_2 < Ni/ZrO_2$ [8]-[14]. Also, Liu *et al.* [15] showed that when the supports of Al_2O_3, CeO_2 and ZrO_2 were tested at low temperature of CO methanation, catalytic activity of Ni increased according to the order of $Ni/CeO_2 < Ni/ZrO_2 < Ni/\gamma\text{-}Al_2O_3$. The last one presented the best catalytic performance with the highest CH_4 selectivity of 94.5% [15].

In the present study, $\gamma\text{-}Al_2O_3$, TiO_2, SiO_2 were selected as a catalyst support for nickel in CO methanation. Since it is supposed that catalyst support should be an important factor for the preparation of fine species of Ni active catalysts, we tested a pulverization of $\gamma\text{-}Al_2O_3$ prior to precipitation of active metal to $\gamma\text{-}Al_2O_3$ support. This research work described an effect of different supports on nickel distribution and particle size, and also an influence of nano milling of $Ni/\gamma\text{-}Al_2O_3$ support on catalytic performances for CO methanation.

2. Experimental Method

Pulverization of γ-Al₂O₃ support prior to precipitation of Ni catalyst

Pulverization of $\gamma\text{-}Al_2O_3$ was carried out using a high energy planetary ball mill described in Figure 1(a), Figure 1(b). A planetary ball mill (HPM-700, Haji Engineering, Korea), as shown in Figure 1(a), was used to grind the samples in this study. Ball milling process is a mechanical process which relies on an energy released at the point of collision between balls as well as on the high grinding energy created by friction of balls on the wall. As shown in Figure 1(b), zirconia balls with 5 mm of diameter were placed in a sintered corundum container. When the mill rotates, balls are picked up by mill wall and rotate around the wall due to centrifugal force leading to grinding of material due to frictional effect. There is also reverse rotation of disc with respect to mill which applies centrifugal force in opposite direction leading to transition of balls on opposite walls
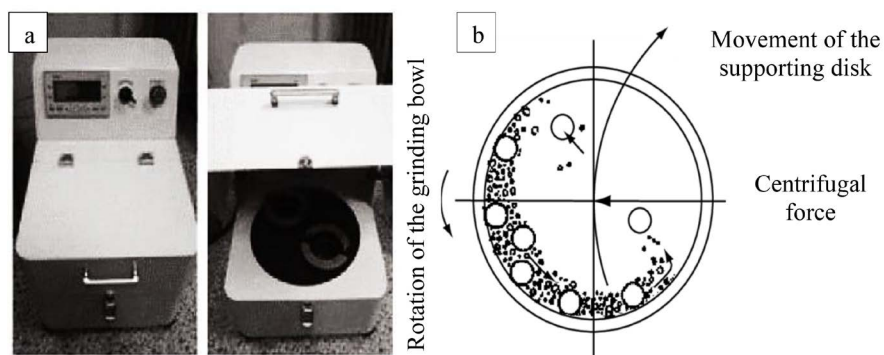
Figure 1. Photo of mill (a) and working principle of ball milling process (b).

of mill. The zirconia ball to sample weight ratio was 10:1. A rotation speed of the planet carrier was 500 rpm. The pulverization of γ-Al_2O_3 was performed for 10 min of dry milling.

Catalyst precipitation method

The different supported Ni catalysts were prepared by impregnation-precipitation method [16] [17] [18]. Initially, catalyst support was dissolved in deionized water of 100 ml. The suspension was heated to 50°C and maintained at that temperature for 30 min. Amount of 10.11 g of $Ni(NO_3)_2 \cdot 6H_2O$ as a nickel precursor was dissolved in 300 ml of deionized water. A slight excess stoichiometrically of Na_2CO_3 aqueous solution with a volume of 300 ml was added dropwise (pH ≈ 9) to the previous solution for precipitation. After stirring continuously for another 1 h at 50°C, the carbonate precipitate was removed by filtration, then it is washed by deionized water three times. Then, the precipitate was dried overnight at 110°C, followed by heating to 500°C with a ramp rate of 2°C/min for calcination in air for 4 h. The catalysts were denoted as Ni/γ-Al_2O_3, Ni/γ-Al_2O_3* (nano), Ni/TiO_2, Ni/SiO_2. All catalysts were pressed into pellets, and then they were further crushed into particles of 45 - 90 mesh, and their activities were evaluated in CO methanation.

Evaluation of catalyst performance

Catalytic test for CO methanation was carried out in a stainless steel tubular reactor with the inner diameter of 8 mm. About 1 g catalyst was used for each test. Catalysts were activated in a hydrogen flow of 13 ml/min at 400°C with a heating rate of 5°C/min for 2 h. After activation, a feed syngas with a volume ratio of $3H_2$:1CO was introduced to the reactor, and its flow rate was controlled by an MFC. Methanation was performed at pressure of 3 bar and with a GHSV of 3000 h^{-1} in the temperature of 350°C. Gas products were separated through a cooler, and analyzed online by a gas chromatography (GC; YL-6100) with a thermal conductivity detector (TCD). The CO conversion, CH_4 yield and selectivity were calculated using the following Equations (3)-(5), respectively.

CO conversion:

$$X_{CO}\left(\%\right) = \frac{V_{CO,inlet} - V_{CO,outlet}}{V_{CO,inlet}} \times 100 \qquad (3)$$

Methane selectivity:

$$S_{CH_4}(\%) = \frac{V_{CH_4,outlet}}{V_{CH_4,outlet} + V_{CO_2,outlet} + V_{H_2,outlet}} \times 100 \tag{4}$$

Methane yield:

$$Y_{CH_4}(\%) = \frac{X_{CO} \times S_{CH_4}}{100} \tag{5}$$

Catalyst characterizations

BET surface area was measured by nitrogen adsorption at the liquid nitrogen temperature on a Flowsorb III 2305/2310 analyzer. Prior to analysis, the samples were degassed under dynamic vacuum at 150°C for 30 min.

XRD measurement was carried out on a mini Flex 600 diffractometer with a monochromatic Co Kα radiations source (λ = 1.7903). The scans were performed from 5° to 95° of 2θ angle with a step size of 0.02°.

Nickel contents in fresh catalysts were determined using by 6500 ICP-OES analyzer.

SEM images were obtained on the JEOL JSM 7001F microscope operated at 10 - 20 kV. The sample was fixed on a carbon black holder with conductive adhesives.

3. Results and Discussion

After the impregnation-precipitation, actual contents of nickel catalysts were measured using a method of ICP-OES. Table 1 shows the nominal and experimental contents of nickel metal precipitated on the different supports by the impregnation-precipitation method.

It was identified that when nickel content of the catalysts was nominally expected as 20 wt%, the obtained contents were between in approximately 17 - 18 wt% depending on different supported catalysts.

Catalyst activity of the Ni/γ-Al$_2$O$_3$* catalyst was compared with those of Ni/γ-Al$_2$O$_3$, Ni/TiO$_2$ and Ni/SiO$_2$ in Figure 2. Activities of the obtained catalysts prepared on different supports were examined at the reaction temperature of 350°C under the syngas pressure of 3 bar.

It was found that Ni/SiO$_2$ catalyst gave the best activity at the equilibration temperature of 350°C, and the CH$_4$ yield reached 85.7%. However, the nano-Ni/γ-Al$_2$O$_3$* catalyst produced a methane from the lowest temperature fitted around 35 minutes of time on stream. This catalyst gave the CH$_4$ yield of 78.7% at the equilibration temperature of 350°C. As shown in Figure 2, the activity of Ni/TiO$_2$ was similar to that of Ni/γ-Al$_2$O$_3$.

Table 2 compared the methane yield and the initial temperature of its formation. The initial temperature of methane formation increased according to the order of Ni/γ-Al$_2$O$_3$* < Ni/SiO$_2$ < Ni/γ-TiO$_2$ < Ni/γ-Al$_2$O$_3$. The Ni/γ-Al$_2$O$_3$* produced methane from the lowest temperature of 178°C to 350°C in CO methanation.
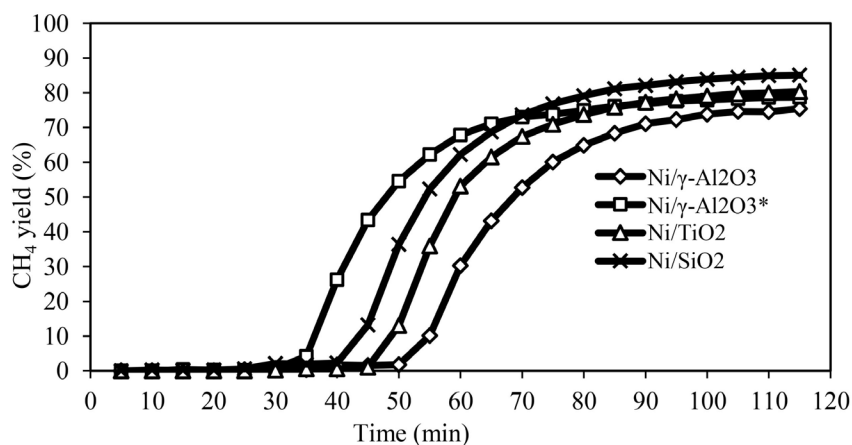
Table 1. Nickel contents after precipitation on the different supports by an impregnation-precipitation method.

Catalyst code	Support	Ni content, (wt %)	
		Nominal	Experimental[1]
Ni/γ-Al$_2$O$_3$	γ-Al$_2$O$_3$	20	17
Ni/γ-Al$_2$O$_3$* (nano)	γ-Al$_2$O$_3$	20	18
Ni/TiO$_2$	TiO$_2$	20	17
Ni/SiO$_2$	SiO$_2$	20	18

[1]Determined by ICP-OES analysis.

Table 2. Comparison of CO methanation performance for Ni/γ-Al$_2$O$_3$, Ni/γ-Al$_2$O$_3$*, Ni/TiO$_2$ and Ni/SiO$_2$ catalysts.

Catalyst code	CH$_4$ yield, %	Initial temperature of CH$_4$ formation, ˚C
Ni/γ-Al$_2$O$_3$	75.4	268
Ni/γ-Al$_2$O$_3$* (nano)	78.7	178
Ni/TiO$_2$	80.4	250
Ni/SiO$_2$	85.7	218

Figure 2. Methane yield obtained during synthesis with the catalysts prepared on different supports.

Activity of Ni/γ-Al$_2$O$_3$* prepared with support pulverization was higher than that of traditional Ni/γ-Al$_2$O$_3$, and the CH$_4$ yield reached 78.7%.

Figure 3 shows that the Ni/γ-Al$_2$O$_3$* catalyst converts almost fully the carbon monoxide into methane. In the end of reaction, the content of CO was only 0.62 % in product gas.

With decreasing the CO content in a feed gas, the methane yield is increasing sharply from 30 minutes to 60 minutes of time on stream, then it was slowly increasing at the equilibration temperature of 350˚C. Regarding temperature program, methanation temperature reaches the equilibration temperature around 60 minutes of time on stream.

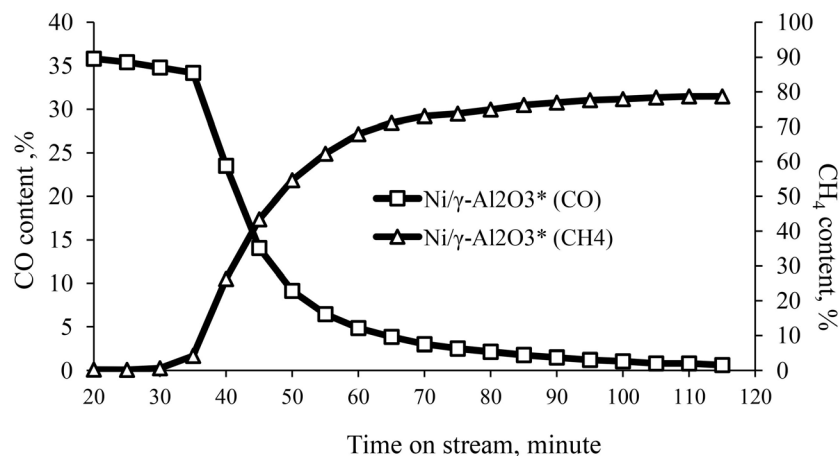**Figure 4** shows the CH$_4$ productivities, which were calculated by a sum of

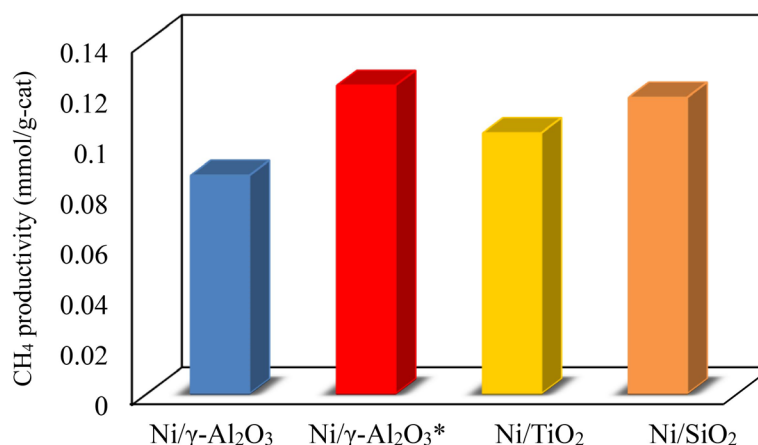**Figure 3.** CO and CH$_4$ contents during methanation synthesis with the Ni/γ-Al$_2$O$_3$*.

Figure 4. CH$_4$ productivities of Ni/γ-Al$_2$O$_3$, Ni/γ-Al$_2$O$_3$*, Ni/TiO$_2$ and Ni/SiO$_2$ catalysts in CO methanation at 350°C.

produced CH$_4$ amount per unit of catalyst weight for 1 h methanation, with the Ni/γ-Al$_2$O$_3$, Ni/γ-Al$_2$O$_3$*, Ni/TiO$_2$ and Ni/SiO$_2$ catalysts in CO methanation at 350°C. It was known that the Ni/γ-Al$_2$O$_3$* catalyst produced the highest amount of methane (0.1224 mmol/g-cat) for 1 h methanation among the four catalysts. However, the traditional Ni/γ-Al$_2$O$_3$ catalyst gave the lowest amount of methane (0.0867 mmol/g-cat) for 1 h methanation, although it contains the same amount of nickel catalyst as that in the Ni/γ-Al$_2$O$_3$* catalyst prepared using the nano milled γ-Al$_2$O$_3$ support. The structures of the two compared catalysts were further analyzed by SEM and XRD analysis.

The SEM images of Ni/γ-Al$_2$O$_3$ and Ni/γ-Al$_2$O$_3$* catalysts are shown in **Figure 5(a)** and **Figure 5(b)**. As shown in **Figure 5(a)**, there were large crevices and cracks, which were illustrated by dark part of SEM image, on the surface of Ni/γ-Al$_2$O$_3$. However, **Figure 5(b)** shows a uniform porous structure illustrated by bright part for metal oxides in the SEM without any large cracks and crevices. It suggests a formation of fine Ni nanoparticles distributed on the surface of nano milled γ-Al$_2$O$_3$* support. The porous structure of the last support provided
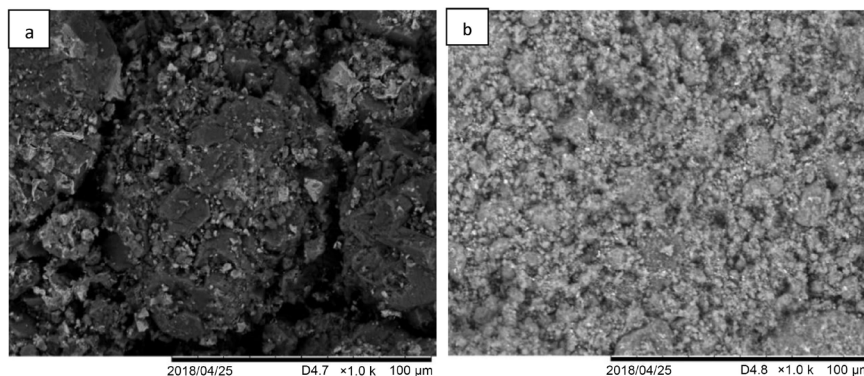
Figure 5. SEM images of the fresh catalysts: (a) Ni/γ-Al$_2$O$_3$ and (b) Ni/γ-Al$_2$O$_3$*.

the good dispersion of active nickel catalyst leading to high activity and selectivity for methane. **Figure 6** describes the X-ray diffractograms of the fresh catalysts of Ni/γ-Al$_2$O$_3$, Ni/γ-Al$_2$O$_3$*, Ni/TiO$_2$ and Ni/SiO$_2$ before methanation process.

The characteristic diffraction peaks of γ-Al$_2$O$_3$ support and NiO appear at 53.55° and 79.59°; and at 43.45°, 50.63° and 74.43°, respectively for the fresh catalysts [16] [17] [18]. For all catalysts prepared by the impregnation-precipitation method, no nickel aluminate species, which were inactive catalytically and non-reducible ones formed by strong interactions between nickel particles and catalyst support, were created in the catalysts. For the Ni/SiO$_2$ catalyst, two broad diffraction peaks in 2θ region of 15.5° - 30.0° were attributed to the diffraction characteristics of amorphous SiO$_2$. For the Ni/TiO$_2$ catalyst, the peaks in 2θ region of 25.3°, 43.8°, 55.0° were attributed to the anatase phase of TiO$_2$. The particle sizes were calculated from the Scherrer formula (6) based on the peak width at 50.63° reflection. The results are listed in **Table 3**. Intensity of the peak at 50.63° of NiO species in Ni/γ-Al$_2$O$_3$ was the strongest among other catalysts, even though their nickel contents were similar (see **Figure 7**). Its NiO particle size calculated by the Scherrer equation was the largest of 21 nm among other catalysts. Moreover, **Table 3** shows the smaller particles of nickel oxides in Ni/γ-Al$_2$O$_3$*, Ni/TiO$_2$ and Ni/SiO$_2$ catalysts.

$$\tau = \frac{K * \lambda}{\beta * \cos\theta} \tag{6}$$

τ—Particle size

K— Shape factor

λ— X-ray wavelength

β—half the maximum intensity (FWHM)

θ—Bragg angle

For the Ni/γ-Al$_2$O$_3$* and the Ni/γ-Al$_2$O$_3$ catalysts, a surface area of catalyst was smaller for the catalyst prepared on the nano milled support of γ-Al$_2$O$_3$. It might be suggested that more fine particles of NiO species filled inside porous structure of the nano milled support.

Figure 8 shows the X-ray diffractograms of the used Ni/γ-Al$_2$O$_3$, Ni/γ-Al$_2$O$_3$*,

Table 3. BET surface area and NiO particle size of the fresh catalysts of Ni/γ-Al$_2$O$_3$, Ni/γ-Al$_2$O$_3$*, Ni/TiO$_2$ and Ni/SiO$_2$.

Catalyst code	S$_{BET}$ (m^2/g)	NiO particle size[1] (nm)
Ni/γ-Al$_2$O$_3$	131	21
Ni/γ-Al$_2$O$_3$* (nano)	115	5
Ni/TiO$_2$	23.1	14
Ni/SiO$_2$	110	<5

[1]Calculated from the peak width at 50.63˚ using Scherrer equation from XRD.
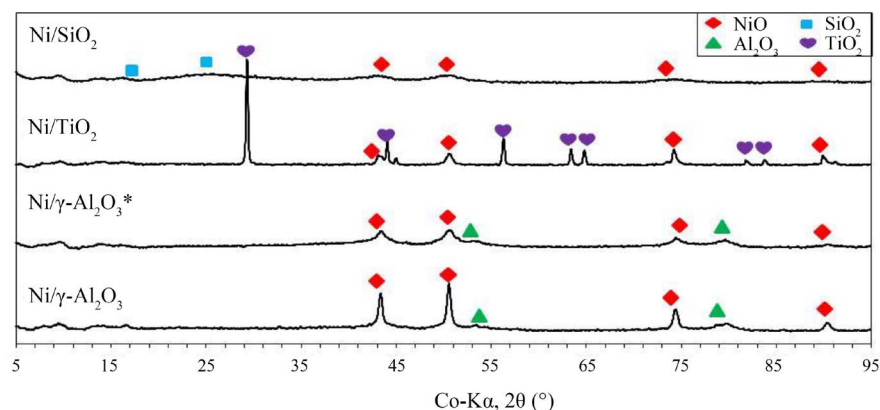
Figure 6. X-ray diffractograms of the obtained catalysts of Ni/γ-Al$_2$O$_3$, Ni/γ-Al$_2$O$_3$*, Ni/TiO$_2$ and Ni/SiO$_2$.
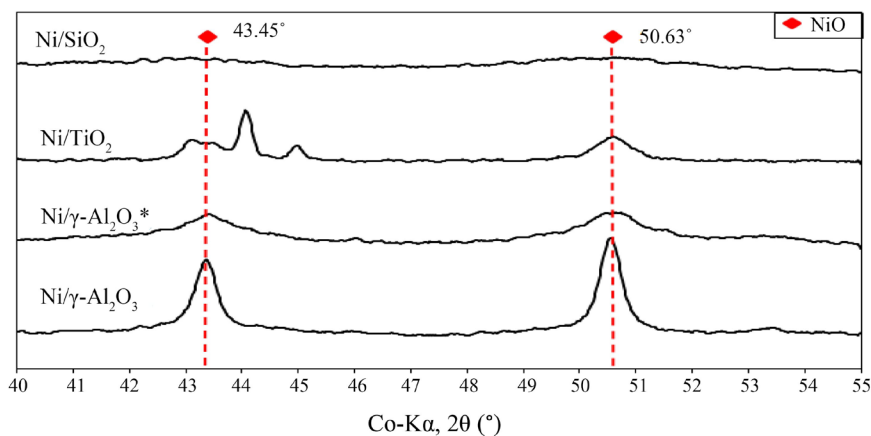
Figure 7. X-ray diffractograms of NiO particles in the Ni/γ-Al$_2$O$_3$, Ni/γ-Al$_2$O$_3$*, Ni/TiO$_2$ and Ni/SiO$_2$.

Ni/TiO$_2$ and Ni/SiO$_2$ catalysts after methanation for 1h at 350˚C. It was known that NiO particles were converted to metal Ni (peaked around at 50.6˚ and 60.9˚) by hydrogen activation for all catalysts, and there were no compounds of nickel catalysts formed due to catalyst deactivation caused by interaction between metal and support during activation and methanation. As shown in **Figure 8**, it was also identified that crystallinity of metallic Ni was very sharp for only the Ni/γ-Al$_2$O$_3$. It might depend on easy agglomeration of large nickel particles in the Ni/γ-Al$_2$O$_3$ in the present reaction conditions.
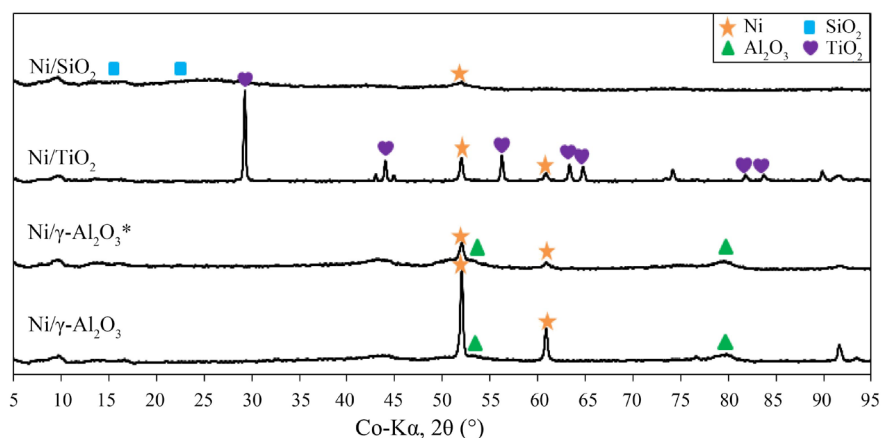
Figure 8. X-ray diffractograms of the used Ni/γ-Al₂O₃, Ni/γ-Al₂O₃*, Ni/TiO₂ and Ni/SiO₂ catalysts after methanation for 1 h.

It is noticeable that the metallic Ni peak at 50.6° of Ni/γ-Al₂O₃* catalyst is smaller than Ni/γ-Al₂O₃, implying that the pulverization of γ-Al₂O₃ improved the dispersion of traditional Ni/γ-Al₂O₃ catalyst.

4. Conclusions

1) The initial temperature of methane formation increased according to the order of Ni/γ-Al₂O₃* < Ni/SiO₂ < Ni/γ-TiO₂ < Ni/γ-Al₂O₃. The Ni/γ-Al₂O₃*, which was prepared on the surface of nano milled γ-Al₂O₃ support, produced methane from the lowest temperature of 178°C to 350°C in CO methanation.

2) The Ni/γ-Al₂O₃* catalyst gave the highest amount of methane (0.1224 mmol/g-cat) for 1 h methanation among other catalysts of the traditional Ni/γ-Al₂O₃, Ni/SiO₂ and Ni/γ-TiO₂.

3) XRD and SEM analysis proved that NiO particles in the Ni/γ-Al₂O₃* were finely distributed, and their sizes were smaller compared to those in the traditional one. The pulverization of γ-Al₂O₃ improved the dispersion of catalytic active nickel species inside porosity of the support leading to the improvement of its catalytic performance.

Conflicts of Interest

The authors declare no conflicts of interest regarding the publication of this paper.

References

[1] Ronsch, S. (2016) Review on Methanation: From Fundamentals to Current Projects. *Fuel*, **166**, 276-296. https://doi.org/10.1016/j.fuel.2015.10.111

[2] Kohei, U., Yuta, T., Yuta, N., Ryuji, K. and Shigeo, S. (2013) Effects of Preparation Conditions of Ni/TiO₂ Catalysts for Selective CO Methanation in the Reformate Gas. *Fuel*, **452**, 174-178. https://doi.org/10.1016/j.apcata.2012.06.021

[3] Shen, D. and Cheng, C. (2017) Methanation of Syngas (H₂/CO) over the Difference Ni-Based Catalysts. *Fuel*, **189**, 419-427. https://doi.org/10.1016/j.fuel.2016.10.122

[4]   Schilidhauer, T.J. (2010) Production of Synthetic Natural Gas (SNG) from Coal and Dry Biomass: A Technology Review from 1950 to 2009. *Fuel*, **89**, 1763-1783. https://doi.org/10.1016/j.fuel.2010.01.027

[5]   Song, I.K. (2012) Hydrogenation of Carbon Monoxide to Methane over Mesoporous Nickel-M-Alumina (M = Fe, Ni, Co, Ce, and La) Xerogel Catalysts. *Journal of Industrial and Engineering Chemistry*, *Fuel*, **18**, 243-248. https://doi.org/10.1016/j.jiec.2011.11.026

[6]   Max-Michael, W., *et al.* (2008) Walter Lurgi's Methanation Technology for Production of SNG from Coal. Ulrich Berger Lurgi.

[7]   Zhang, J., *et al.* (2014) Low-Temperature Methanation of Syngas in Slurry Phase over Zr-Doped Ni/γ-Al$_2$O$_3$ Catalysts Prepared Using Different Methods. *Fuel*, **132**, 211-218. https://doi.org/10.1016/j.fuel.2014.04.085

[8]   Baowang, L. and Katsuya, K. (2013) Preparation of the Highly Loaded and Well-Dispersed NiO/SBA-15 for Methanation of Producer Gas. *Fuel*, **103**, 669-704. https://doi.org/10.1016/j.fuel.2012.09.009

[9]   Mengdie, C., Jie, W., Wei, C., Xueqing, C. and Li, Z.J. (2011) Methanation of Carbon Dioxide on Ni/ZrO$_2$-Al$_2$O$_3$ Catalysts: Effects of ZrO$_2$ Promoter and Preparation Method of Novel ZrO$_2$-Al$_2$O$_3$ Carrier. *Fuel*, **20**, 318-324. https://doi.org/10.1016/S1003-9953(10)60187-9

[10]   Takenaka, S., Shimizu, T. and Otsuka, K. (2004) Complete Removal of Carbon Monoxide in Hydrogen-Rich Gas Stream through Methanation over Supported Metal Catalysts. *International Journal of Hydrogen Energy*, **29**, 1065-1073. https://doi.org/10.1016/j.ijhydene.2003.10.009

[11]   Andrigo, P., Bagatin, R., Pagani, G., *et al.* (1999) Fixed Bed Reactor. *Catalyst Today*, **52**, 197-221. https://doi.org/10.1016/S0920-5861(99)00076-0

[12]   Hoekman, S.K. and Broch, A. (2010) CO$_2$ Recycling by Reaction with Renewably Generated Hydrogen. *International Journal of Greenhouse Gas Control*, **4**, 44-50. https://doi.org/10.1016/j.ijggc.2009.09.012

[13]   Mohseni, F. and Magnusson, M. (2012) Biogas from Renewable Electricity: Increasing a Climate Neutral Fuel Supply. *Applied Energy*, **90**, 11-16. https://doi.org/10.1016/j.apenergy.2011.07.024

[14]   Barelli, L., Bidini, G., Gallorini, F. and Servili, S. (2008) Hydrogen Production through Sorption-Enhanced Steam Methane Reforming and Membrane Technology: A Review. *Energy*, **33**, 554-570. https://doi.org/10.1016/j.energy.2007.10.018

[15]   Liu, Z., Chu, B. and Zhai, X. (2012) Total Methanation of Syngas to Synthetic Natural Gas over Ni Catalyst in a Micro-Channel Reactor. *Fuel*, **9**, 559-605. https://doi.org/10.1016/j.fuel.2011.12.045

[16]   Buyan-ulzii, B., Daariimaa, O., Munkhdelger, C., Oyunbileg, G. and Enkhsaruul, B. (2018) Effect of Nickel Precursor and Catalyst Activation Temperature on Methanation Performance. *Mongolian Journal of Chemistry*, **19**, 12-18. https://doi.org/10.5564/mjc.v19i45.1084

[17]   Barsbold, K., Buyan-ulzii, B. and Enkhsaruul, B. (2018) Carbon Monoxide Methanation: Effect of Catalyst Preparation Method. *Journal of Mongolian Chemical Society*, **13**, 50-62.

[18]   Buyan-ulzii, B., Oyunbileg, G. and Enkhsaruul, B. (2018) Carbon Monoxide Methanation: Effect of Catalyst Preparation Method. *Fossil Fuel Chemistry*, *Processing and Ecology Issue*, *Ulaanbaatar*, **6**, 21-29.